An Algorithm for the Solution of Impurity Diffusion under Finite Reaction Rates

K. Lackner, K. Behringer, W. Engelhardt, and R. Wunderlich
Max-Planck-Institut für Plasmaphysik, Garching bei München

Z. Naturforsch. **37a**, 931–938 (1982); received May 19, 1982

To Professor Arnulf Schlüter on his 60th Birthday

An algorithm allowing a fast solution of stationary and time dependent 1-d diffusion problems for the case of finite ionization and recombination rates is presented. Results of numerical computations and an analytic stability analysis show its unconditional stability. The computational effort involved rises only linearly with the number of ionization stages included. An application to the diffusion of oxygen and iron impurities in JET is described.

1. Introduction

The solution of the finite rate equations of impurity diffusion in a tokamak is of crucial importance both for the interpretation of experimentally observed distributions of impurity ion species in terms of transport models (e.g. [1]), and for a realistic assessment of the potential of radiating boundary layers as a means of energy transfer to the walls (see [2] and references cited there). So far respective algorithms have proven usually to be too time-consuming to allow inclusion into general simulation codes and large-scale production runs. A limited number of full-scale discharge simulations, including the finite-rate effects, have recently been reported by Mercier et al. [3].

Aiming at an interpretation of Pulsator [4] and ASDEX [1] impurity distribution measurements, Behringer and Engelhardt have been successful with using a relatively simple algorithm (called BE in the following) for the treatment of both the stationary and the time-dependent problem, resulting in a computational effort increasing only linearly with the number of ionic stages included in the computations. This was achieved by treating recombination only as perturbation term, computed explicitly from the results of the preceding iteration or time step. Intuition, test calculations, and the results of a stability analysis in Sect. 4 show that this is indeed a valid method in cases dominated by diffusion and ionization, but has to run into numerical difficulties when approaching coronal equilibrium or other situations with important contributions from recombination.

This observation suggests a more symmetric treatment of ionization and recombination, which can be realized by alternating in successive steps between ionization and recombination as the terms treated explicitly or implicitly. The resulting algorithm (WL) conserves the advantageous scaling of the computational effort with the number of included ionization stages, and has been shown unconditionally stable for all combinations of diffusion, ionization and recombination time constants. It is described, together with test calculations for simplified model systems, in Sect. 2 as a solution method to the stationary, and in Sect. 3 to the time-dependent problem. Section 4 describes the analytic stability analysis for the BE and WL algorithms, confirming the conclusions of the numerical tests. Finally, we report results of calculations for a realistic system under conditions in the range expected for the JET experiment (Sect. 5) and compare the present method with alternative existing algorithms (Section 6).

2. Algorithm for the Stationary Problem

For outlining the algorithms we use a simple diagonal diffusion model with spatially constant coefficients and slab geometry. This should be a valid approach for testing stability properties; the additional complexities arising under realistic conditions are discussed in Section 5. The stationary system we then can write in matrix notation as

$$\mathbf{D}\frac{\mathrm{d}^2}{\mathrm{d}x^2}\boldsymbol{n} = \mathbf{S}\cdot\boldsymbol{n} + \mathbf{R}\cdot\boldsymbol{n} - \boldsymbol{d} \qquad (1)$$

Reprint requests to Max-Planck-Institut für Plasmaphysik, Bibliothek, D-8046 Garching.

0340-4811 / 82 / 0800-0931 $ 01.30/0. — Please order a reprint rather than making your own copy.

with **D** a diagonal matrix and $\boldsymbol{n}$, **S**, **R** and $\boldsymbol{d}$ vectors and matrices in the space of ionization stages

$$\boldsymbol{n} = \begin{pmatrix} n_1 \\ n_2 \\ \cdot \\ \cdot \\ \cdot \\ \cdot \\ n_K \end{pmatrix}, \quad \mathbf{S} = \begin{pmatrix} s_1 & 0 & 0 & \cdots & & & \\ -s_1 & s_2 & 0 & \cdots & & & \\ 0 & -s_2 & s_3 & \cdots & & & \\ \cdot & \cdot & \cdot & \cdots & & & \\ & & & \cdot & & & \\ & & & & \cdot & \cdot & \cdot \\ & & & & \cdot & s_{K-1} & 0 \\ & & & & 0 & -s_{K-1} & s_K \end{pmatrix},$$

$$\mathbf{R} = \begin{pmatrix} r_1 & -r_2 & 0 & \cdots & & & \\ 0 & r_2 & -r_3 & \cdots & & & \\ 0 & 0 & r_3 & \cdots & & & \\ \cdot & \cdot & \cdot & \cdots & & & \\ & & & \cdot & & & \\ & & & & \cdot & \cdot & \cdot \\ & & & & \cdot & r_{K-1} & -r_K \\ & & & & \cdot & 0 & r_K \end{pmatrix}.$$

For simplicity we have absorbed here the electron density into the ionization and recombination rates s_j and r_j, respectively.

Using a diffusion-type model only for the ionized stages (n_j being j-times ionized), the ionization of neutral impurities is contained in the source term $\boldsymbol{d}$, which therefore has the form

$$\boldsymbol{d} = \begin{pmatrix} +d(x) \\ 0 \\ 0 \\ 0 \\ \cdot \\ \cdot \\ \cdot \\ 0 \end{pmatrix}.$$

For the following we assume $d(x)$ to be a given function (for the tests reported in this section, e.g. $d(x) = (\nu + 1)\, x^{\nu}$).

The difference formulation of (1) is rather similar to that of a two-dimensional diffusion equation. Due to the structure of the **R** and **S** matrices, the ionization and recombination terms of the system look like a discrete analogon to a diffusion equation (with inhomogeneous coefficient) in the coordinate of the ionization state.

Engelhardt [4] has successfully applied the iteration scheme

$$\mathbf{D}\frac{\mathrm{d}^2}{\mathrm{d}x^2}\boldsymbol{n}^l - \mathbf{S}\boldsymbol{n}^l = \mathbf{R}\boldsymbol{n}^{l-1} - \boldsymbol{d}, \qquad \text{(BE 1a), (WL 1a)}$$

where l refers to the iteration cycle. Including at the new level only ionization allows, due to the structure of the S-matrix, to solve successively the diffusion equation for the ionization degrees in increasing order, using a standard algorithm for tridiagonal matrices.

An extension to this, rendering the treatment symmetric in **R** and **S** consists in following each such step by another one of the form

$$\mathbf{D}\frac{\mathrm{d}^2}{\mathrm{d}x^2}\boldsymbol{n}^{l+1} - \mathbf{R}\boldsymbol{n}^{l+1} = \mathbf{S}\boldsymbol{n}^l - \boldsymbol{d}. \qquad \text{(WL 1b)}$$

This modification conserves the advantage that again the equation for different ionization degrees can be solved one after the other, albeit here now in descending order.

Results of numerical tests of these two schemes are reported in more detail in [5]. The system tested corresponds to a simple model, with the absolute magnitude of all non-zero elements of the three matrices **D**, **S**, **R** equal to constants D_0, S_0, R_0, respectively. The character of the system then changes with the relative magnitudes of three time constants which are defined by

$$\tau_D = (D_0/(L)^2)^{-1}, \quad \tau_S = S_0^{-1} \quad \text{and}$$
$$\tau_R = R_0^{-1},$$

where L is the dimension of the system. Cases reported there correspond to ratios

$$\tau_D : \tau_S : \tau_R = (1:0.1:1), \quad (1:1:0.1),$$
$$(1:0.1:0.1), \quad (1:0.05:0.05),$$
$$(1:0.01:0.01).$$

The system used contained only four ionization stages; boundary conditions for the test were

$$\left.\begin{array}{ll} \text{at} & x = 0 : (\mathrm{d}/\mathrm{d}x)\, n_j = 0 \\ \text{at} & x = L = 1 : n_j \;\; = 0 \end{array}\right\} \text{for all ionization stages.}$$

Whereas the method alternating in the implicit treatment of ionization and recombination was found to converge throughout (and even for more extreme parameter combinations like $(1:10^{-3}:10^{-3})$, the unidirectional BE method failed in the case $(1:1:0.1)$ corresponding to dominating recombination rate, and when approaching coronal equilibrium situations $(1:10^{-2}:10^{-2})$.

3. Algorithm for the Time-Dependent Problem

Both for assistance in diagnostic interpretation of impurity injection experiments and as a potential component of 1-d simulation calculations, time-dependent calculations are of even greater practical importance. The system under otherwise identical assumptions to those of (1) and using the same notation then reads

$$\frac{\partial}{\partial t}\boldsymbol{n} - \mathbf{D}\frac{\partial^2}{\partial x^2}\boldsymbol{n} = -\mathbf{S}\cdot\boldsymbol{n} - \mathbf{R}\cdot\boldsymbol{n} + \boldsymbol{d}. \quad (2)$$

Behringer and Engelhardt have used an algorithm including a Crank-Nicholson description of the diffusion term of the form

$$\frac{1}{\Delta t}(\boldsymbol{n}^l - \boldsymbol{n}^{l-1}) - \theta\,\mathbf{D}\frac{\partial^2 \boldsymbol{n}^l}{\partial x^2} + \mathbf{S}\cdot\boldsymbol{n}^l \quad \begin{matrix}(\text{BE } 2),\\ (\text{WL } 2\text{a})\end{matrix}$$
$$= (1-\theta)\,\mathbf{D}\frac{\partial^2 \boldsymbol{n}^{l-1}}{\partial x^2} - \mathbf{R}\cdot\boldsymbol{n}^{l-1} + \boldsymbol{d}^{l-1/2}$$

with θ the usual constant deciding the degree of time-centering of the spatial derivatives, the index l now referring to a time-step.

The corresponding "symmetrized" version consists in alternating such a time-step, with one of the form

$$\frac{1}{\Delta t}(\boldsymbol{n}^{l+1} - \boldsymbol{n}^l) - \theta\,\mathbf{D}\frac{\partial^2 \boldsymbol{n}^{l+1}}{\partial x^2} + \mathbf{R}\cdot\boldsymbol{n}^{l+1}$$
$$= (1-\theta)\,\mathbf{D}\frac{\partial^2 \boldsymbol{n}^l}{\partial x^2} - \mathbf{S}\cdot\boldsymbol{n}^l + \boldsymbol{d}^{l+1/2}. \quad (\text{WL } 2\text{b})$$

Again, by proceeding either up- or downwards the scale of ionization stages, the resulting difference equations can be solved by a usual routine for tridiagonal systems.

Test runs using the time-dependent WL-algorithm were carried out under similar simplifying assumptions and over the same range of parameter combinations (τ_D, τ_R, τ_S) as described in Sect. 2, using a time-step $\Delta t = 10(\Delta x)^2/D_0$. Results, presented in more detail in [5] showed the stability of the method. Comparison calculations using 4-byte and 8-byte accuracy gave a relative deviation of less than 2×10^{-4} in the concentration of the fully ionized state for a system with 16 ionization stages and 48 grid points, proving also a relative insensitivity to round-off errors.

4. Analytic Stability Analysis for the Time Dependent Algorithm

The favourable stability properties of the scheme described by the equations WL2a + WL2b can also be ascertained by an amplification factor analysis like outlined e.g. in [6]. The only non-standard part of it consists a Fourier decomposition of the errors $\delta\boldsymbol{n}$ also with regard to the ionization stage, writing

$$\delta n_j^{l-1}(x) = \sum_{m=0}^{\infty}\sum_{k=1}^{K} N_{m,k} \cdot \exp\left\{i\pi k\frac{j}{K}\right\}\exp\left\{i\pi m\frac{x}{L}\right\}.$$

The amplification factor of the step WL2a (= BE2) for the m, k error component $N_{m,k}$ can then be computed as

$$\gamma_{\text{BE}} = \frac{1 + (1-\theta)c - 2\left(\sin\pi\frac{k}{2K}\right)^2 R_0\Delta t + 2i R_0\Delta t \sin\pi\frac{k}{2K}\cos\pi\frac{k}{2K}}{1 - \theta c + 2\left(\sin\pi\frac{k}{2K}\right)^2 S_0\Delta t + 2i S_0\Delta t\sin\pi\frac{k}{2K}\cos\pi\frac{k}{2K}} \quad (3)$$

with c as an abbreviation of the term

$$c = 2\left(\cos\left(\pi m\frac{\Delta x}{L}\right) - 1\right)\cdot D_0\frac{\Delta t}{(\Delta x)^2} \quad (4)$$

known from the analysis of the Crank Nicholson scheme. For error damping in this simple repeated algorithm (the BE scheme), we require

$$\gamma_{\text{BE}}\,\gamma_{\text{BE}}^* = \frac{(1+(1-\theta)c)^2 - 4(1+(1-\theta)c)\,R_0\Delta t\left(\sin\pi\frac{k}{2K}\right)^2 + 4(\Delta t)^2 R_0^2\left(\sin\pi\frac{k}{2K}\right)^2}{(1-\theta c)^2 + 4(1-\theta c)\cdot S_0\Delta t\left(\sin\pi\frac{k}{2K}\right)^2 + 4(\Delta t)^2 S_0^2\left(\sin\pi\frac{k}{2K}\right)^2} < 1$$

over the whole range of

$$-2<\cos\left(\pi m\frac{\Delta x}{L}\right)-1<0\,,\quad 0<\sin^2\left(\pi\frac{k}{K}\right)<1$$

which for arbitrary values of Δt is the case only for $R_0<S_0$ and $\theta\gtrsim 0.5$.

For the symmetrized, two step algorithm (WL scheme) the amplification factor over a whole cycle reads

$$\gamma_{\mathrm{WL}}=\frac{\eta_1^2-2(\eta_1\Delta t(R_0+S_0)-2(\Delta t)^2R_0S_0)\left(\sin\pi\frac{k}{2K}\right)^2+2i\eta_1\Delta t(R_0-S_0)\sin\pi\frac{k}{2K}\cos\pi\frac{k}{2K}}{\eta_2^2+2(\eta_2\Delta t(R_0+S_0)+2(\Delta t)^2R_0S_0\left(\sin\pi\frac{k}{2K}\right)^2-2i\eta_2\Delta t(R_0-S_0)\sin\pi\frac{k}{2K}\cos\pi\frac{k}{2K}} \tag{5}$$

with the abbreviations

$$\eta_1=1+(1-\theta)c\,,\quad \eta_2=1-\theta c\,.$$

As $\eta_2>0$ and $|\eta_1|<|\eta_2|$, from this expression follows stability for $\theta\gtrsim 0.5$ for all values of Δt and independent of the relative magnitude of R_0 and S_0.

5. Applications to Impurity Transport Calculations for Tokamaks

Conditions for physically realistic situations differ considerably from the assumptions of the model system used in the previous section. Tokamak transport is generally analysed in cylindrical symmetry and the profiles of electron density and temperature provide for a very strong variation of the components of **R** and **S** over the radius r. Moreover, neoclassical theory and attempts for empirical fitting of measurements lead to the introduction of additional terms in the relation between impurity fluxes and densities and density gradients.

For dimensions and operating conditions of present and future tokamak devices and low and medium Z impurities nearly all ionization stages will be concentrated in a near boundary region which will emit under these conditions also the major part of the total radiation. In an even thinner boundary layer, the neutral impurities entering the plasma will be ionized defining thereby the spatial extent of the source term $\boldsymbol{d}(x)$ introduced in Section 2. For these reasons it seems mandatory to use a spatially inhomogenous grid with greatly enhanced resolution in the outer layers.

For the code version used for the following test calculations we have taken account of this necessity by formulating and solving the differential equation system in terms of a coordinate $\varrho=r^\alpha$ using a constant grid spacing $\Delta\varrho$ and exponents α typically 2 or 3. In this coordinate the cylindrical impurity diffusion equations reads

$$\varrho^{2/\alpha-1}\cdot\frac{\partial\boldsymbol{n}}{\partial t}-\alpha^2\frac{\partial}{\partial\varrho}\varrho\mathbf{D}\frac{\partial}{\partial\varrho}\boldsymbol{n}+\alpha\frac{\partial}{\partial\varrho}\varrho^{1/\alpha}\mathbf{v}\cdot\boldsymbol{n}=-\varrho^{2/\alpha-1}(\mathbf{S}\cdot\boldsymbol{n}+\mathbf{R}\cdot\boldsymbol{n}+\boldsymbol{d})\,, \tag{6}$$

where we have introduced a diagonal matrix **v** to describe additional (drift-type) terms arising from empirical assumptions or neoclassical theory.

A minor problem asises in the formulation of the boundary condition at $\varrho=0$, as the usual expression $(\partial/\partial r)\,n_j=0$ cannot be transformed into a useable expression in ϱ (for $\alpha>1$) because of

$$\frac{\partial}{\partial\varrho}n_j=(\varrho^{1/\alpha-1}/\alpha)\frac{\partial}{\partial r}n_j\,.$$

The boundary condition at $r=0$ for the cylindrical equation can be understood, however, as the absence of a singular source term at the centre. The total flux of species n_j through a surface of radius r and of unit length in cylindrical direction, which is given by $2\pi r(-D_j(\partial n_j/\partial r)+v_j n_j)$ therefore has to satisfy

$$\lim_{r\to 0}r\left(D_j\frac{\partial n_j}{\partial r}-v_j n_j\right)=\lim_{r\to 0}\sigma_j\frac{r^2}{2}$$

with an unspecified constant σ_j. In the coordinate ϱ this condition translates into

$$\lim_{\varrho\to 0}\left(\alpha D_j\varrho\frac{\partial n_j}{\partial\varrho}-\varrho^{1/\alpha}v_j n_j\right)=\lim_{\varrho\to 0}\sigma_j\frac{\varrho^{2/\alpha}}{2}=0$$
$$\text{for all}\quad \alpha>0\,,$$

which can be conveniently incorporated into the system when placing the first interior grid point at $\varrho=\frac{1}{2}\Delta\varrho$.

Test calculations to be reported here were carried out for an equivalent JET geometry with $a = 1.62$ m and assumed electron density and temperature profiles of the form

$$n_e(r) = n_e(0)\,(0.9 \cdot (1 - (r/a)^2) + 0.1) \quad \text{and}$$
$$T_e(r) = (T_e(0) - 10\,\text{ev})\,(1 - (r/a)^2)^2 + 10\,\text{ev}.$$

A simple diffusion law, compatible with ASDEX measurements [1], was chosen, with $D = 0.5\ \text{m}^2/\text{s}$ $v = -(r/a)\ v_0$ for all species. The boundary condition at $r = a$ was of the form

$$-\mathbf{D}\frac{\partial}{\partial r}\boldsymbol{n} + \mathbf{v}\cdot\boldsymbol{n} = v_{\text{eff}}\cdot\boldsymbol{n}$$

with an effective outflow velocity $v_{\text{eff}} = 50$ m/s.

The source of charged particles $\mathrm{d}(r)$ was determined by ionization of a given flux density of neutral impurity atoms Γ_0 streaming radially inward with the average thermal velocity corresponding to 3 ev. The inflow was kept constant for 2 sec and then suddenly switched off; calculations were then continued for a further 1 sec. Initial conditions were $n_j(r) \equiv 0$ for all stages.

Calculations were performed for two impurity species (oxygen and iron) using also different diffusion models, flux rates, background plasma parameters and exponents for the radial coordinates.

Case A (oxygen):

$$v_0 = 0, \quad \Gamma_0 = 10^{17}\,\text{m}^{-2}\,\text{s}^{-1},$$
$$n_e(0) = 3 \times 10^{19}\,\text{m}^{-3}, \quad T_0(0) = 1000\,\text{ev},$$
$$\alpha = 3;$$

case B (iron):

$$v_0 = 1\ \text{ms}^{-1}, \quad \Gamma_0 = 10^{16}\,\text{m}^{-2}\,\text{s}^{-1},$$
$$n_e(0) = 5 \times 10^{19}\,\text{m}^{-3}, \quad T_e(0) = 5000\,\text{ev},$$
$$\alpha = 2.$$

The grid contained 50 interior points equidistant in ϱ; transformed into r, the grid point distance varied therefore between 23 and 1.6 cm in the iron and 44 and 1 cm in the oxygen case. Each calculation was done with three different time steps (10 ms, 5 ms, 1 ms); the corresponding stability parameter $\Delta t \cdot D/(\Delta r)^2$ for the longest time step varied therefore between 0.1 (at the centre) and 20 (at the boundary) in the iron, and between 0.025 and 50 in the oxygen case.

Results are shown in figures 1 a and b in the form of the radial distribution of the total impurity content and of the single ionic stages at $t = 2$ s, immediately before the switching off of the impurity flow, and in Figs. 2 a and b for the time behaviour of the fully stripped stage at the innermost grid point. In the absence of an inward drift term the total impurity content tends asymptotically in time towards $\sum n_j = \text{const}$ over the whole source-free region (see Fig. 1 a), whereas the transport model used for the iron case produces a peaked profile $\sum n_j \sim \exp(-v_0 r^2/(a \cdot D))$ interior to the ionization layer.

None of the calculations showed any indication of numerical instability. A comparison of the results obtained with $\Delta t = 10$ ms and $\Delta t = 1$ ms gave a deviation in the total impurity concentration (a measure of the accuracy in the solution of the diffusion part of the system) $\delta \sum n_j / \sum n_j$ of 6×10^{-3} at the centre and of 3×10^{-4} at the 45th grid point. The deviations in the relative concentrations of the single ionic species $\delta(n_j/\sum n_j)$ were much smaller, reaching even for iron only 4×10^{-4} in the locally dominating stage and becoming $< 10^{-6}$ for stages constituting only a minority (e.g. Fe XXII at the centre).

Sudden changes in parameters of the calculation like the start with a finite impurity influx rate or the discontinuity of the latter at $t = 2$ s cause perturbations in the calculation which, because of the stable nature of the difference scheme, are damped out with time. This is illustrated in Figs. 3 a and b using the maximum negative ion species density appearing anywhere over the grid as a measure of such a perturbation. Comparison of the results with the different Δt values shows that this damping is clearly a function of the number of time steps as the magnitude of the largest negative number for $\Delta t = 0.01$ s (Fig. 3 a) at 2 s is nearly the same as for $\Delta t = 10^{-3}$ s (Fig. 3 b) at 0.2 s. This suggests, of course, to use a variable time step, reducing it during phases with rapidly changing parameters.

Values given in Figs. 3 a and b refer to the profiles obtained after a step with implicit treatment of the ionization term. Figure 3 c gives the corresponding values taken after a step with implicit treatment of the recombination term, for $\Delta t = 10^{-3}$ s: the negative numbers show a similarly damped behaviour, but a nearly 3 orders of magnitude larger amplitude. This is indeed to be expected because the magnitude of the elements of **S** is far larger than that of **R** over most of the plasma

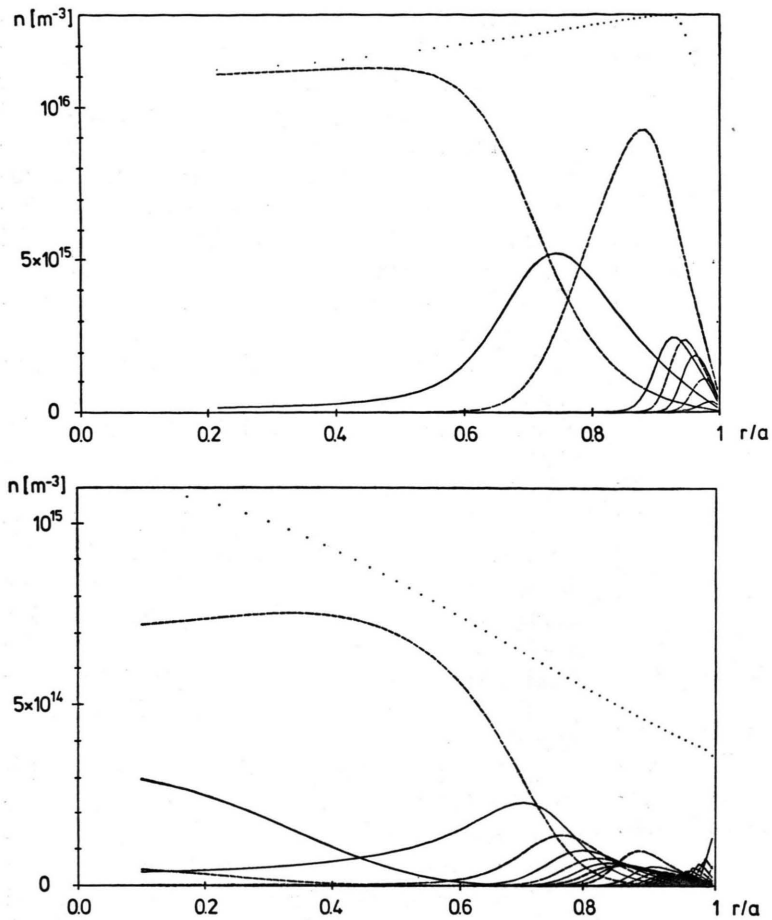

a)

b)

Fig. 1. Density profiles at $t=2$ s for the oxygen (Fig. 1a) and iron (Fig. 1b) test cases described in Section 5. Dashed and solid lines are used for even and add ionization stages, respectively (in spectroscopic notation); the dotted line gives the total density $\sum n_j$.

cross-section, with **R** dominating only in the outer zones. As a consequence of this, we use only the profiles obtained after a step with implicit treatment of ionization for the evaluation of physics quantities, with the step containing implicit treatment of recombination serving only for stabilization of the whole system.

The CPU computer times required for these calculations covering a 3 s interval were 1.88, 2.91 and 11.1 s on a CRAY 1 computer for the oxygen cases

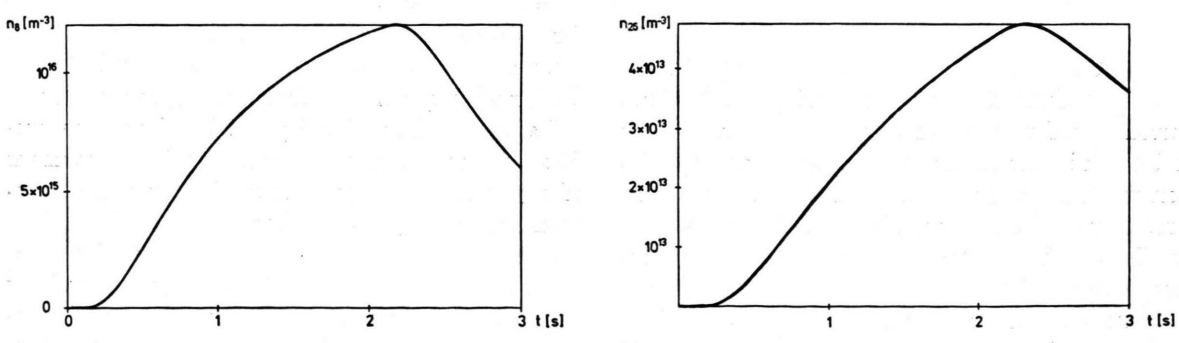

a) b)

Fig. 2. Time behaviour of the density of the fully ionized stage at the innermost grid point for the oxygen (Fig. 2a) and iron (Fig. 2b) test cases of Section 5.

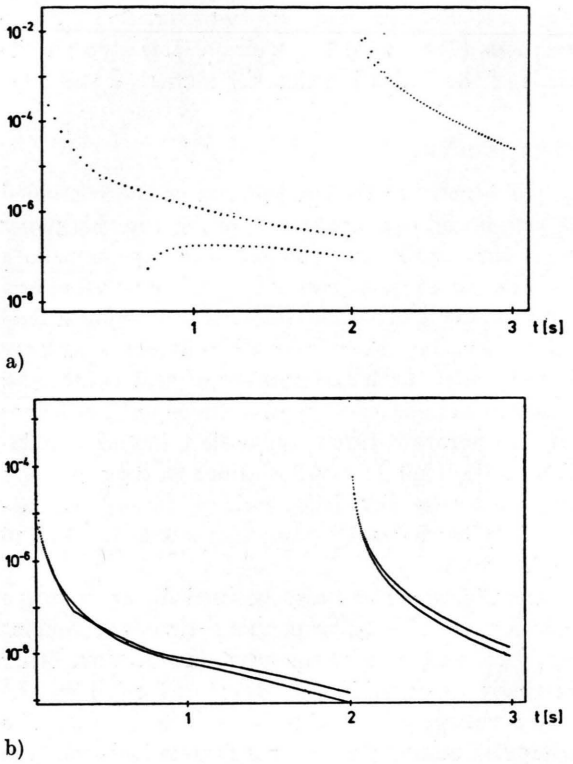

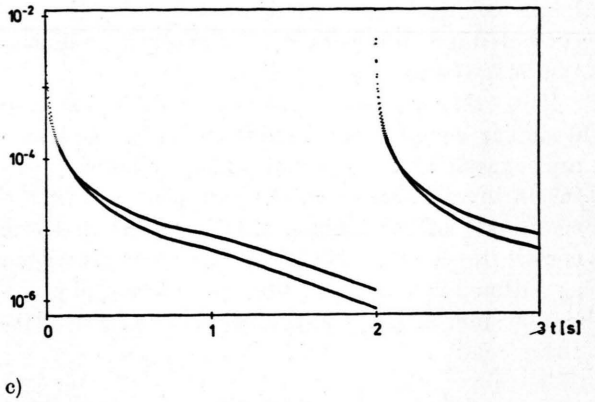

Fig. 3. Damping of numerical fluctuations excited by discontinuities in the prescribed impurity influx for the oxygen case of section 5. Shown is the maximum negative species density appearing anywhere in the system as a function of time, normalized by the volume average total density $\sum n_j$ at $t = 2$ s. Figure (a) and (b) give results after time steps with implicite treatment of ionization, Fig. (c) with implicit treatment of recombination. Time steps used were 10 ms for (a) and 1 ms for (b) and (c).

using $\Delta t = 0.01$, 0.005 and 0.001 respectively, and 3.2, 4.88, 19.2 s for the corresponding iron runs. This corresponds to a needed CPU time of 3.4 ms/time step for oxygen and 5.9 ms for iron. The even less than linear increase in CPU requirement with the number of ionization stages is obviously due to the features of the CRAY computer and the programming, which allowed vectorization of the calculations only for the intermediate ionization stages but treated separately the first and the last one.

6. Alternative Solution Methods

Other methods for the solution of the combined impurity diffusion and rate equation have been described and applied by the authors of refs. [7], [8], [3].

The method of Okamoto and Amano consists in a time-splitting technique, solving the diffusion part of the equations by a Crank-Nicholson scheme and the rate equations as an eigenvalue problem. The computational effort involved in the latter step is quite large and increases quadratically with the number of ionization stages involved, so that the method has so far been applied only for stand-alone calculations.

Another possibility consists in considering the difference equations arising from an implicit formulation of the system of Eqs. (6) as a block-tridiagonal matrix. Depending on the arrangement of the variables, the single submatrices will then describe either the diffusion in space or the ionization and recombination effects. In both cases they are also tridiagonal. Direct solution of this system of difference equations proceeds then by the analogue to the Thomas algorithm (see e.g. [6]) involving thereby, however, an inversion of the single submatrices. During this inversion the tridiagonal structure of these submatrices is lost, so that the subsequent operations involve full matrices. The total computational effort will therefore be linear in either the number of ionization stages or of grid points, but quadratic in the other dimension [8]. The same system of difference equations could also be solved by a SOR technique making use of the sparseness of the system. This was done in the calculations described in [3]; comparison calculations have shown, however, that this technique requires a factor of two

larger computer time per time-step, than the one presented in this paper for a test case with 8 ionization stages and 25 grid points.

Two other methods, requiring for each time step a similar computational effort as the present one, are suggested by the formal similarity between diffusion in real space and the rate processes in the coordinate of the ionization stages. The first one constitutes a direct complement to our algorithm as outlined in Section 3. For the differential equation system used there, the two steps of this algorithm read

$$\frac{1}{\Delta t}(\boldsymbol{n}_i^l - \boldsymbol{n}_i^{l-1}) + \mathbf{S}\cdot\boldsymbol{n}_i^l + \mathbf{R}\cdot\boldsymbol{n}_i^l + \mathbf{D}\frac{\boldsymbol{n}_i^l - \boldsymbol{n}_{i-1}^l}{\Delta x} = \mathbf{D}\frac{\boldsymbol{n}_{i+1}^{l-1} - \boldsymbol{n}_i^{l-1}}{\Delta x} + \boldsymbol{d}_i^{l-1/2}, \tag{7a}$$

$$\frac{1}{\Delta t}(\boldsymbol{n}_i^{l+1} - \boldsymbol{n}_i^l) + \mathbf{S}\cdot\boldsymbol{n}_i^{l+1} + \mathbf{R}\cdot\boldsymbol{n}_i^{l+1} - \mathbf{D}\frac{\boldsymbol{n}_{i+1}^{l+1} - \boldsymbol{n}_i^{l+1}}{\Delta x} = -\mathbf{D}\frac{\boldsymbol{n}_i^l - \boldsymbol{n}_{i-1}^l}{\Delta x} + \boldsymbol{d}_i^{l+1/2}, \tag{7b}$$

where i describes the space index and Δx the grid distance.

The second algorithm consists in a direct application of the alternating direction implicit method (ADI) successful in two-dimensional diffusion problems:

$$\frac{1}{\Delta t}(\boldsymbol{n}^l - \boldsymbol{n}^{l-1}) + \mathbf{S}\cdot\boldsymbol{n}^l + \mathbf{R}\cdot\boldsymbol{n}^l = \mathbf{D}\frac{\partial^2\boldsymbol{n}^{l-1}}{\partial x^2} + \boldsymbol{d}^{l-1/2}, \tag{8a}$$

$$\frac{1}{\Delta t}(\boldsymbol{n}^{l+1} - \boldsymbol{n}^l) - \mathbf{D}\frac{\partial^2\boldsymbol{n}^{l+1}}{\partial x^2} = -\mathbf{S}\cdot\boldsymbol{n}^l - \mathbf{R}\cdot\boldsymbol{n}^l + \boldsymbol{d}^{l+1/2}. \tag{8b}$$

Test calculations showed, however, both these methods (7) and (8) to require a time step on the scale of the ionization time for numerical stability.

7. Conclusions

The algorithm for the solution of the combined diffusion and rate equations outlined in this paper was found stable independently of time step both by analytic examination of a simplified system and by realistic test calculations. The computational effort per time step is small and increased only linearly with both the number of grid points and ionization stages. The speed of the algorithm allows to incorporate it into a full-scale tokamak simulation code, and test calculations adding it as a module to the BALDUR code [9] have been successfully carried out for impurities with Z up to 26 [10].

The algorithm can also be used for an iterative solution of the corresponding time-independent problem. In this case the advantage against other methods — notably the direct inversion of the block-tridiagonal matrix [8] — is less clear. The computational effort required for one iteration step of the present algorithm is, however, comparatively small, so that test calculations have shown it to be competitive or even advantageous also in this case.

Acknowledgements

The authors are grateful to Dr. W. Schneider for carrying out comparison calculations with a code created by his program generator "DEQTRAN" [11]. The physical conditions for the test calculations reported in Sect. 5 have been specified by Dr. M. Watkins and J. Cordey.

[1] K. Behringer, W. Engelhardt, and G. Fußmann, IAEA Technical Committee Meeting on Divertor and Impurity Control, Garching 1981, paper I.C. 6.
[2] K. Lackner and J. Neuhauser, ibid, paper II. R2.
[3] C. Mercier, F. Werkoff, J. P. Morera, C. Cissoko, and H. Capes, Nucl. Fusion **21**, 291 (1981).
[4] W. Engelhardt, Bull. Amer. Phys. Soc. **22**, 1106 (1977).
[5] K. Lackner, K. Behringer, W. Engelhardt, and R. Wunderlich, IPP Report IPP 1/195, Garching 1981.
[6] R. D. Richtmeyer and K. W. Morton, Difference Methods for Initial-Value Problems, Interscience Publishers, New York 1967.
[7] M. Okamoto and T. Amano, J. Comp. Phys. **26**, 80 (1978).
[8] R. Hulse, private communication.
[9] D. E. Post et al., TFTR Physics Group Report **33**, Princeton Plasma Physics Lab., USA, 1981.
[10] J. Neuhauser et al., to be published.
[11] D. Düchs and W. Schneider, 2nd European Conf. on Comput. Physics, Garching 1976, paper E5, (Proceeddings IPP 6/147).